Memoirs of the Faculty of Engineering, Okayama University, Vol.31, No. 2, pp.21-27, March 1997

Estimation of Internal Viscoelasticity by Mechanical Impedance

Hisao OKA* and Takahiko NAKAMURA*

(Received February 25, 1997)

SYNOPSIS

In evaluating the stiffness of skin surface, internal structures such as bone and muscle often affect the measurements. In the present paper, acoustic random vibration is used to estimated the viscoelasticity of a silicone-gel model. This viscoelasticity, which includes two different stiffness strata, is first estimated using a mechanical impedance spectrum, which describes the relation between the depth and viscoelasticity of internal objects. This method is applied to the depth of a silicone-gel tumor model measured by ultrasound imaging and the viscoelasticity of internal gel can be accurately estimated.

1. INTRODUCTION

In evaluating the stiffness of skin surface, internal structures such as bone and muscle often affect the measurements and lead to conflicting results. This suggests, conversely, that internal body structures and viscoelasticities can be derived from the skin surface measurements[1].

More commonly, of course, x-ray CT, MRI, SPECT, and ultrasound imaging have been applied to such examinations[2]. These methods have allowed for structural determinations, although ultrasound has also been used to estimated bone density and the movement and function of internal organs.

In the present paper, acoustic random vibration (30-1000Hz) is used to estimated the viscoelasticity of a silicone-gel model. This viscoelasticity, which includes two different stiffness strata, is first estimated using a mechanical impedance spectrum, which describes the relation between the depth and viscoelasticity of internal objects. This method is then applied to an estimation of the viscoelasticity of a silicone-gel tumor model. The experimental silicone-gel tumor model includes two internal hemisphere gels, the stiffness of which is different from that of peripheral silicone-gel. Finally, by applying the relation between depth and viscoelasticity to the depth measured by ultrasound imaging, the viscoelasticity of the internal hemisphere is estimated.

* Department of Electrical and Electronic Engineering

2. MECHANICAL IMPEDANCE

2.1 Measurement system of impedance

Mechanical impedance is defined by force *f(t)* and acceleration *a(t)*, when the vibration forces on a living body.

$$Z(j\omega) = \frac{F(j\omega)}{V(j\omega)} = \frac{F(j\omega)}{A(j\omega)/j\omega} = j\omega\frac{F(j\omega)}{A(j\omega)} \quad \cdots(1)$$

Where $F(j\omega)$ and $A(j\omega)$ are transformed by Fast Fourier Transform from *f(t)* and *a(t)*.

Figure 1 shows a block diagram of measurement system of mechanical impedance. The skin surface is randomly vibrated at 30-1000Hz by the vibrator. The force *f(t)* and acceleration *a(t)* at a driving point are detected by using the impedance-head in the probe. The *f(t)* and *a(t)* are converted from an analog to a digital signal, and input to a personal computer. These signals are transformed by FFT, and then the mechanical impedance spectrum are obtained.

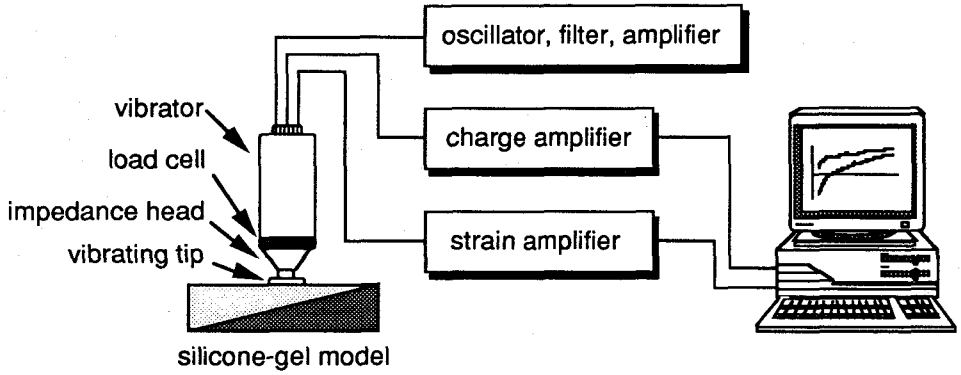

Fig. 1 Measurement system of mechanical impedance.

2.2 Radiation impedance in living tissues

In analysis of wave propagation on living tissues, the viscoelasticity must be considered. Generally, the equation of wave motion in an isotropic, elastic, viscous and compressible medium is expressed as follows[3]:

$$-\rho\omega^2 \boldsymbol{S} = (\mu + \lambda)\, grad\,(div\, \boldsymbol{S}) + \mu \Delta \boldsymbol{S} \quad \cdots(2)$$

where $\mu = \mu_1 + j\omega\mu_2$, $\lambda = \lambda_1 + j\omega\lambda_2$, ρ [kg/m³]: medium density, μ_1 [N/m²]: coefficient of shear elasticity, μ_2 [Ns/m²]: coefficient of shear viscosity, λ_1 [N/m²]: coefficient of volume compressibility, and λ_2 [Ns/m²]: coefficient of volume viscosity.

Equation (2) is expanded by a displacement vector $\boldsymbol{S}$ on an oscillating sphere, and a radiation impedance is as follows:

$$Z = \frac{P}{j\omega S_0} = -\frac{4}{3}\pi\rho\omega a^3 j \frac{\left(1 - \frac{3}{ah}j - \frac{3}{a^2h^2}\right) - 2\left(\frac{1}{ah}j + \frac{1}{a^2h^2}\right)\left(3 - \frac{a^2k^2}{akj+1}\right)}{\left(\frac{1}{ah}j + \frac{1}{a^2h^2}\right)\frac{a^2k^2}{akj+1} + \left(2 - \frac{a^2k^2}{akj+1}\right)} \quad \cdots(3)$$

where *a*[m]: radius of a oscillating sphere, and $h^2 = \rho\omega^2/\mu$ and $k^2 = \rho\omega^2/(2\mu + \lambda)$.
From Eqn. (3), $\lambda_1 = \infty$ and $\lambda_2 = 0$ in an incompressible medium like a living body, and $ak \ll 1$ in

enough low frequency. Then the impedance $Z(j\omega)$ is expressed as follows[4]:

$$Z = -\frac{2}{3}\pi\omega a^3 \rho j\left(1 - \frac{9j}{ah} - \frac{9}{a^2h^2}\right) \quad \cdots(4)$$

2.3 Extension to viscoelasticity

In this study, we treat the mechanical impedance as equal to the radiation impedance of an oscillating sphere in a semi-infinite medium. Then Eqn. (4) is expanded as follows:

$$Z(j\omega) = 6\pi a^2\sqrt{\frac{\rho\left(\sqrt{\mu_1^2+\omega^2\mu_2^2}+\mu_1\right)}{2}} + 6\pi a\mu_2 + j\omega\frac{2\pi a^3\rho}{3} + j6\pi a^2\sqrt{\frac{\rho\left(\sqrt{\mu_1^2+\omega^2\mu_2^2}-\mu_1\right)}{2}} + \frac{6\pi a\mu_1}{j\omega} \quad \cdots(5)$$

A living body is considered a semi-infinite medium as shown in Fig. 2, and so Eqn. (5) is multiplied by 1/2. The mechanical impedance includes three pattern spectra: a soft, stiff, and intermediate pattern, and Eqn. (5) can only be used to express the soft pattern. This spectrum is curve-fitted by the above theoretical Eqn. (5), and then μ_1, μ_2, a and ρ (constant) are obtained.

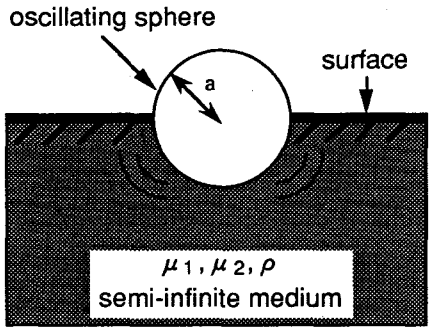

Fig. 2 Oscillating sphere in a semi-infinite medium.

3. VISCOELASTICITY OF SILICONE-GEL

Figure 3 shows silicone-gel slope models for obtaining the relation between the depth and viscoelasticity of silicone-gels that have two different stiffness strata. By palpation, the stiffness of the silicone-gel (Shin-Etsu Chemical Co.,Ltd., Shin-Etsu Silicone, KE1052(A, B)) is similar to that of skin. Figure 3 (a) shows a silicone-gel A model in which the gel A is put on an acrylic slope. This model can be used to obtain the relation between the depth and viscoelasticity of silicone-gel A itself, since the acrylic board is much stiffer than silicone-gel. Figure 3 (b) shows the silicone-gel AB and AC models, in which the gel A is put on the gel B or C slope. The deeper the distance to gel B or C from the gel A surface, the stronger the upper stratum is reflected in viscoelasticity, because the lower stratum is made of silicone-gel. The silicone-gel B is stiffer than gel A, and gel C is softer than gel A. The penetrations of the silicone-gels are as follows: A, 70; B, 50; and C, 90.

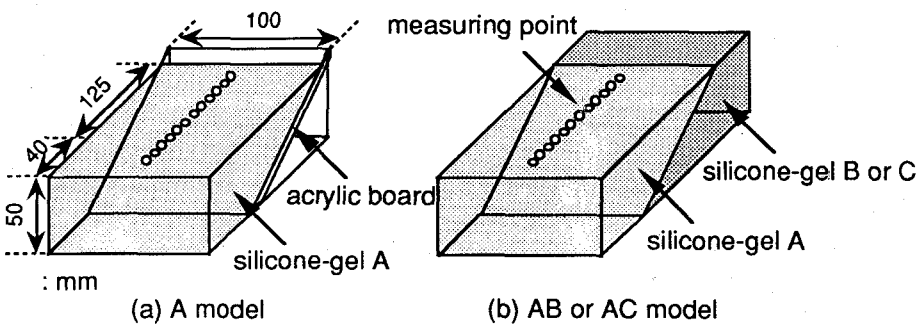

Fig. 3 Silicone-gel slope model.

The mechanical impedance of these models is measured with a space of 5 mm in the direction that the distance to the lower stratum increases. The vibrating disk is 10 mm in diameter, and the contact preload onto the gel surface is 10 gf.

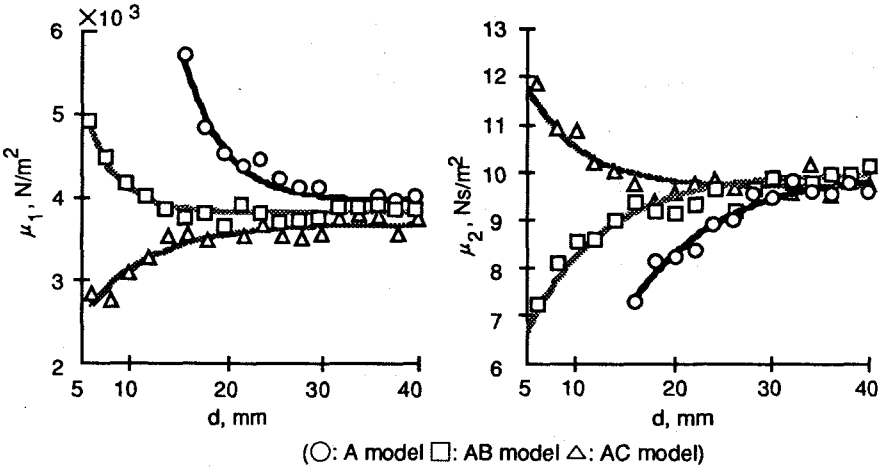

Fig. 4 Relation between depth and viscoelasticity.

The obtained mechanical impedance spectrum is curve-fitted, and the apparent elasticity μ_1 and viscosity μ_2 are calculated. Figure 4 shows the relation between the vertical distance to the lower stratum and the viscoelasticity. That is, the viscoelasticity measured at the model surface is an apparent viscoelasticity due to the influence of the lower stratum. This relationship also shows that the influence of the silicone-gel of the lower stratum is not a factor in cases where the distance to the lower stratum is longer than about 20 mm. It is possible, then, to estimate the viscoelasticity of the lower gel by using this relation, when the distance to the lower stratum is less than about 20 mm.

4. ESTIMATION OF VISCOELASTICITY OF THE TUMOR MODEL

Figure 5 shows a silicone-gel tumor model having two different tumors (Tumor B and Tumor C, the hemispheres of which are made of silicone-gels B and C respectively) in a peripheral silicone-gel A. The diameter of each tumor is 50 mm and the height of each tumor is 40 mm. The mechanical impedance is measured at 540 (15×36) points above the tumor with a latticed space of 5 mm. The vibrating disk is 10 mm in diameter and the contact preload is 10 gf.

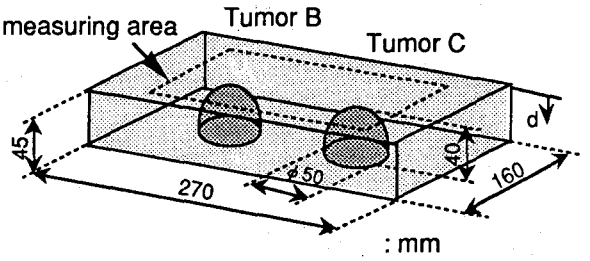

Fig. 5 Silicone-gel tumor model.

4.1 Method of viscoelasticity estimation

It is considered that the viscoelasticity is related to the depth in the case of the silicone-gel model having two strata. This model may be regarded as being coupled in series each other, as shown in Fig. 6.

The viscoelasticity of silicone-gel AB model can be obtained from Eqns. (6) and (7) by expanding the Maxwell model[5].

$$\frac{\alpha_1}{\mu_{1An}} + \frac{\beta_1}{\mu_{1Bn}} = \frac{1}{\mu_1} \qquad \cdots(6)$$

$$\frac{\alpha_2}{\mu_{2An}} + \frac{\beta_2}{\mu_{2Bn}} = \frac{1}{\mu_2} \quad \cdots(7)$$

where μ_{1An} is a convergent elasticity of the silicone-gel AB model (it is regarded as the elasticity of the silicone-gel A itself); μ_{1Bn} is the elasticity of the silicone-gel AB model in the case that d = 0 mm (it is regarded as the elasticity of the silicone-gel B itself); and α_1 and β_1 are weighted coefficients of μ_{1An} and μ_{1Bn}, respectively. The viscosity in Eqn. (7) is similar to that of the elasticity.

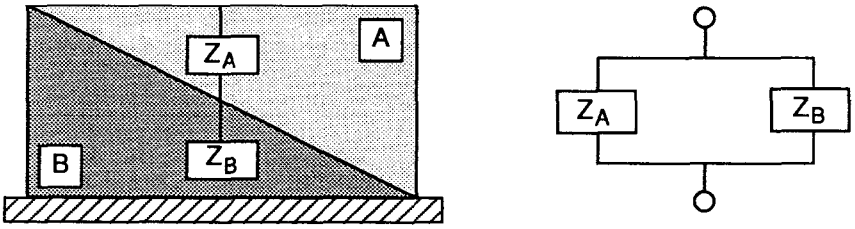

Fig. 6 Mechanical structure of silicone-gel AB model.

4.2 Estimation of viscoelasticity

The internal viscoelasticities of tumors μ_1 and μ_2 are estimated from the measured values. However, it must be considered that these values include the influence of the vibrating area around the measuring point. Figure 7 shows the influence of these surroundings.

The relation between μ_1 and μ_2 and the depth obtained from the silicone-gel slope model (Fig. 4) is as follows:

$$\mu_1 = c_1 + c_2 \exp(-c_3 d) \quad \cdots(8)$$

$$\mu_2 = c_1' + c_2' \exp(-c_3' d) \quad \cdots(9)$$

where c_1, c_2, c_3, c_1', c_2' and c_3' are a positive real number.

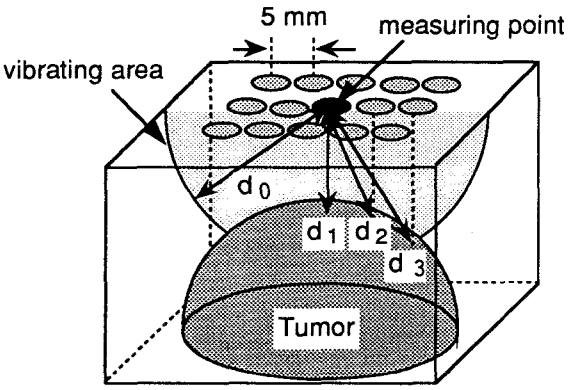

Fig. 7 Influence of surroundings.

Considering the influence of the surroundings, Eqns. (8) and (9) are transformed as follows.

$$\mu_1' = c_1 + c_2 \exp\left[-c_3 d_1 - c_3 \sum_{i=2}^{69} \left\{ \frac{d_i - d_1}{|d_i - d_1|} \frac{d_0 - d_i}{d_0} \frac{d_i}{d_0} \right\}\right] \quad \cdots(10)$$

$$\mu_2' = c_1' + c_2' \exp\left[-c_3' d_1 - c_3' \sum_{i=2}^{69} \left\{ \frac{d_i - d_1}{|d_i - d_1|} \frac{d_0 - d_i}{d_0} \frac{d_i}{d_0} \right\}\right] \quad \cdots(11)$$

Where μ_1' and μ_2' are measured values on a measuring point, and d_0 is a vibrating area in a semi-infinite medium, $(d_i - d_1) / |d_i - d_1|$ expresses a behaviour of surrounding vibration, and $d_0 - d_i$ expresses an expansion of vibration. The vibrating area of surroundings reaches to 68 measuring points because, as shown in Fig. 4, the silicone-gel of lower stratum does not exert an influence at a distance of 20 mm. That is, i is defined as 2 to 69.

The distance to measuring point d_1 is measured using ultrasound imaging, after then d_i and d_0 are calculated. Figure 8 shows a reconstruction of the tumor model by ultrasound imaging (TOSHIBA, SSA-240A). It is measured from the surface of tumor model with a latticed space of 5

mm. When Eqns. (10) and (11) are substituted into Eqns. (8) and (9), μ_1 and μ_2 just under the measuring point are as follows:

$$\mu_1 = c_1 + \frac{\mu_1' - c_1}{exp\left[-c_3 \sum_{i=2}^{\infty} \left\{ \frac{d_i - d_1}{|d_i - d_1|} \frac{d_0 - d_i}{d_0} \frac{d_i}{d_0} \right\}\right]} \quad \cdots(12)$$

$$\mu_2 = c_1' + \frac{\mu_2' - c_1'}{exp\left[-c_3' \sum_{i=2}^{\infty} \left\{ \frac{d_i - d_1}{|d_i - d_1|} \frac{d_0 - d_i}{d_0} \frac{d_i}{d_0} \right\}\right]} \quad \cdots(13)$$

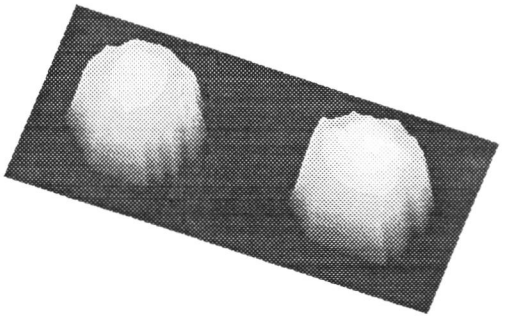

Fig. 8 Reconstruction of tumor model by ultrasound imaging.

The relation curve between μ_1 and μ_2 under the measuring point and the depth measured by the ultrasound imaging is curve-fitted by Eqns. (6) and (7), and α and β are obtained.

Considering the internal hemisphere silicone-gel B, the obtained μ_{1An}, α_1, β_1 and the measured value μ_1 of tumor model are substituted into Eqn. (6). The elasticity of internal hemisphere silicone-gel B, μ_{1Bn}, is obtained at each measuring point. Elasticities are obtained for internal hemisphere silicone-gel C, μ_{1Cn} in a similar way. The viscosities, μ_{2Bn} and μ_{2Cn}, of the internal tumor are also obtained in this fashion. Figure 9 shows the estimated elasticity of hemisphere silicone-gel, which is obtained from smoothing μ_{1Bn} and μ_{1Cn} by the V-Filter. The figure also shows a vertical cross-section in the middle of the estimated figure. As shown in Fig. 9, the elasticity of hemisphere silicone-gel B is higher than that of peripheral gel A, and that of hemisphere gel C is lower. Figure 10 shows the estimated viscosity of the hemisphere silicone-gels. The viscosity of hemisphere gel B is lower, and that of hemisphere gel C is higher, than peripheral gel A.

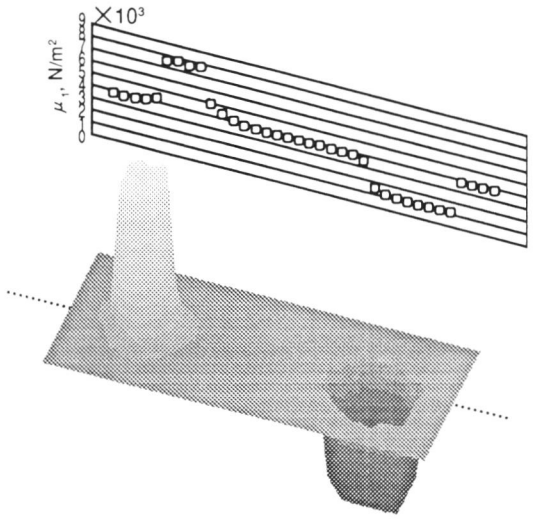

Fig. 9 Estimated elasticity of hemisphere silicone-gel.

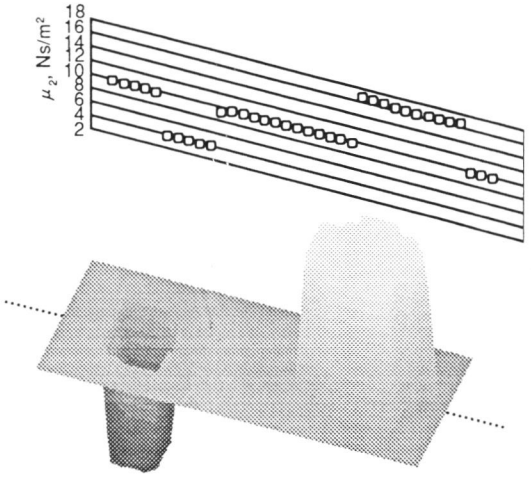

Fig. 10 Estimated viscosity of hemisphere silicone-gel.

4.3 Discussion

As shown in Figs. 9 and 10, the viscoelasticity between the internal tumor and peripheral silicone-gel A is quite different. Table 1 shows the measured and estimated viscoelasticity of hemisphere silicone-gel (considering, not considering the influence of surroundings) and a standard deviation. It is clear that when the estimated viscoelasticities of silicone-gels B and C of the model are derived under consideration of the surroundings, they are closer to the measured values than when derived without such consideration.

Table 1 Estimation of viscoelasticity.

	Tumor B			Tumor C		
	measured	estimated		measured	estimated	
		not considering	considering		not considering	considering
μ_1 [N/m^2]	8677	6464 ±97	7383 ±798	1299	3082 ±166	1421 ±295
μ_2 [Ns/m^2]	3.75	7.68 ±0.85	4.58 ±0.68	15.02	11.19 ±0.09	16.82 ±0.15

5. CONCLUSIONS

In this study, the viscoelasticity of internal silicone-gel is estimated with the relation between the depth to internal gel and the measured viscoelasticity. The relation between the depth and viscoelasticity is obtained by measuring the mechanical impedance of silicone-gel slope model and by an ultrasound imaging. This method is applied to the silicone-gel tumor model and the viscoelasticity of internal gel can be accurately estimated.

REFERENCES

(1) T. Irie, H. Oka, K. Yasuhara and T. Yamamoto: Development of a hardness-meter for the human body, Trans. IEE Japan, 112-C(8)(1992), 443, 450.

(2) J. R. Cameron and J. G. Skofronick: Medical Physics, John Wiley & Sons, Inc., New York, (1978)

(3) H. L. Oestreicher: Field and Impedance of an Oscillating Sphere in a Viscoelastic Medium with an Application to Biophysics, J. Acoust. Soc. Am., 23(6)(1951), 707, 714.

(4) H. E. von Gierke, H. L. Oestreicher, E. K. Franke, H. O. Parrack and W. W. von Wittern: Physics of Vibrations in Living Tissues, J. Appl. Physiol., 4(1952), 886, 900.

(5) H. Oka, T. Fukuda, S. Sakamoto, T. Nakamura and M. Yasuna: Estimation of Body Constitution with Mechanical Impedance, Tech. Re. IEICE, MBE 94-46(1994), 53, 60.